Predictive modeling of ionic permselectivity of porous media

Libor Seda, Juraj Kosek

ICT Prague, Department of Chemical Engineering, 166 28 Prague 6, Czech Republic

Abstract

Transport and separation processes in ionic systems located in the porous medium are investigated. The software for the modeling of the combined electroosmotic, migration, diffusion and pressure driven flow in the spatially 2D or 3D porous medium has been developed. This software allows to determine the mapping from the parametric space of the porous structure and distribution of fixed charge into the space of application properties such as ionic permselectivity or perfusion flow. Software capabilities are illustrated on case studies of systems where the Debye length is either comparable or negligible with respect to the characteristic pore size. The concept of the reconstructed porous medium has been employed to represent the morphology.

Keywords: ionic system, permselectivity, reconstructed porous media, electroosmotic flow, concentration polarization.

1. Introduction

Porous media of various types are involved in practical applications involving ionic electrolytes, e.g., capillary electrochromatography (CEC), nanofiltration, electrodialysis, fuel cells and other membrane applications. One of the important practical problems is to find the relation between the micro-structure of porous media, the distribution of concentrations of ions and the electroosmotic flow through the porous media. Another practical problem is the prediction of the permselectivity of membranes from their known structure, from the distribution of fixed charge in the membrane and from the concentration of the electrolyte. We have applied the methodology of the reconstructed porous medium and employed the solution of the Navier-Stokes, Poisson and mass balance equations to address the above mentioned problems.

The previous attempts to describe and model the electroosmotic flow ingeneral porous media followed one of three principal methodologies forced by computational feasibility and/or introduced idealization of the original system: (i) digitally reconstructed porous media with negligible Debye length [1], (ii) network models of inter-connected cylindrical pores [2], and (iii) reduction to effective-scale (averaged) 1D-models or models with simple geometry, such as 2D cylindrical model [3].

2. Reconstructed porous medium

Spatial distribution of phases can be represented in the general case by the so called phase function $f_i: \mathbb{R}^3 \to \{0;1\}$ for each phase *i*. The phase function of the pore phase is defined as [4]

$$f_g(\mathbf{r}) = \begin{cases} 1 & \text{if } \mathbf{r} \in \text{pore}, \\ 0 & \text{otherwise}. \end{cases}$$
 (1)

340 L. Seda and J. Kosek

By definition only one phase can be present at any point $r \in \mathbb{R}^3$. In a discrete form the phase function $f_g(r)$ becomes the phase volume function which assigns each finite volume element of space (voxel) a value from the set $\{0;1\}$. In a practical implementation the domain on which the phase volume functions are specified is typically a cubic grid of $N_x \times N_y \times N_z$ voxels, cf. Figure 1. Such a region of real space is called the computational unit cell. The relationship between the unit cell and the porous medium of interest depends on the absolute dimensions of the medium and on the spatial resolution at which the medium is represented (feature dimensions). The unit cell can either contain the entire medium plus some void space surrounding it, or be a sample of a much larger (theoretically infinite) medium. In the latter case the dimensions of the unit cell must be such that the unit cell is statistically representative of the entire medium.

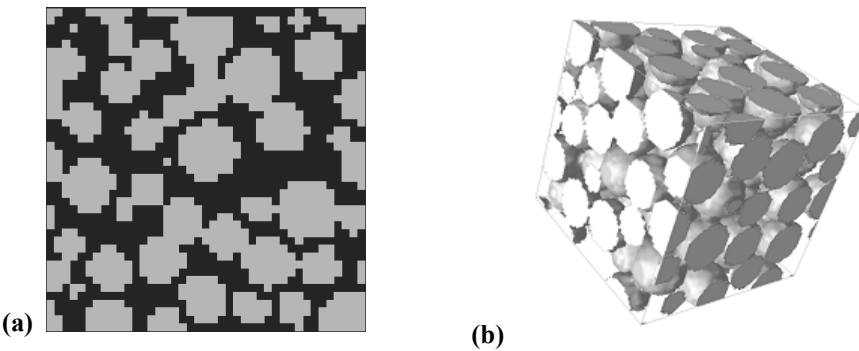


Figure 1. (a) Porous slot, section of Fig. 1b.; black color is pore and blue color is solid. (b) Reconstructed granular medium. Periodic boundary conditions.

The reconstruction of the porous/multi-phase medium is the process starting from the image obtained by the electron microscopy or by other imaging techniques, followed by the evaluation of the suitable morphological descriptors of the image, and concluding by the generation of the spatially 3D porous/multi-phase medium with the same morphological characteristics as those of the original image. In mathematical terms, given the porosity and the suitable morphological characteristics, we want to reconstruct the replica of the porous medium represented by the phase function $f_g(\mathbf{r})$ defined on the discrete grid of voxels with coordinates \mathbf{r} . The overview of several algorithms of the stochastic or diagenetic reconstruction of the porous media is available in [5]. The reconstructed porous medium is then used as the input for the calculation of effective transport, mechanical and electric properties of the medium [6], or as the input for the modeling of various reaction, transport and transformation processes.

3. Model equations

Stationary distributions of velocity and pressure for the incompressible liquid are obtained by the solution of the continuity and Navier-Stokes equations

$$\nabla \cdot \mathbf{v} = 0,$$

$$\rho(\mathbf{v} \cdot \nabla \mathbf{v}) = -\nabla p + \eta \nabla^2 \mathbf{v} - q \nabla \phi,$$
(1)

where v is the velocity, ρ is the density, p is the pressure, η is the dynamic viscosity, q is the charge density and ϕ is the electric potential. The term $(-q\nabla\phi)$ is the electric force acting on the unit volume of the fluid. The charge density q is the linear combination of concentrations of ions c_i ,

$$q = F \sum_{i} z_i c_i , \qquad (2)$$

where F is the Faraday constant and z_i is the charge number of the i-th species. Local electroneutrality assumption (q = 0) usually holds in the bulk electrolyte far from charged surfaces.

In the system with the Debye length comparable with the characteristic pore size, the distribution of the electric potential is obtained from Poisson equation

$$\nabla^2 \phi = -q / (\varepsilon_r \varepsilon_0) \,, \tag{3}$$

where ε_r and ε_0 are the relative and absolute permittivity.

The steady state local balance of species i in the ionic system without chemical reaction is considered in the form

$$\nabla \cdot \boldsymbol{J}_{i} = 0, \quad \text{with} \quad \boldsymbol{J}_{i} = \boldsymbol{v}\boldsymbol{c}_{i} - D_{i}\nabla\boldsymbol{c}_{i} - F/(RT)\boldsymbol{z}_{i}D_{i}\boldsymbol{c}_{i}\nabla\phi, \quad (4)$$

where J_i is the molar flux intensity of the *i*-th species defined by the Nernst-Planck equation, D_i is the diffusivity of the *i*-th species, R is the gas constant and T is the temperature. The balance (4) is considered for all species, i = 1, ..., N.

The system of equations (1)–(4) with appropriate boundary conditions for the set of state variables $\{p, v, \phi, q, c_i\}$ is solved. The boundary conditions at the surface of the solid phase are

$$\mathbf{n} \cdot \mathbf{v} = 0$$
, $\mathbf{n} \cdot \nabla \phi = \sigma / (\varepsilon_r \varepsilon_0)$, $\mathbf{n} \cdot \mathbf{J}_i = 0$, $i = 1,...,N$, (5)

where n is the local outer unit normal vector of the solid phase and σ is the surface charge density. The conditions on the boundary of the computational domain depend on the considered case: (i) boundary conditions (5) are applied for the impermeable wall with immobilized zero or non-zero surface charge density, (ii) Dirichlet boundary conditions, or (iii) periodic boundary conditions. For example, Dirichlet boundary conditions on the left and right boundary of the computational domain are

left boundary:
$$p = p_{\text{left}}$$
, $\phi = \phi_{\text{left}}$, $c_i = c_{i,\text{left}}$, $i = 1,...,N$, right boundary: $p = p_{\text{right}}$, $\phi = \phi_{\text{right}}$, $c_i = c_{i,\text{right}}$, $i = 1,...,N$. (6)

When the Debye length is negligible when compared to the characteristic pore size, e.g., in the case of highly concentrated electrolytes, the grid required to solve the model equations (1)–(4) in the vicinity of the solid phase with a non-zero surface charge density σ would have to be very fine. In an alternative approach the very thin electric double layer is excluded from the computational domain, so the electric term $(-q\nabla\phi)$ in eq (1) is not considered and local electroneutrality assumption (q=0) holds in the electrolyte. The set of state variables reduces to $\{p, v, \phi, c_i\}$, and the system is described by the modified eqs (1'), (2') and by eqs (4),

$$\nabla \cdot \mathbf{v} = 0,$$

$$\rho(\mathbf{v} \cdot \nabla \mathbf{v}) = -\nabla p + \eta \nabla^2 \mathbf{v},$$
(1')

$$0 = F \sum_{i} z_i c_i , \qquad (2)$$

and the boundary conditions at the surface of the solid phase change to

$$\boldsymbol{n} \cdot \boldsymbol{v} = 0$$
, $\boldsymbol{t} \cdot \boldsymbol{v} = -\mu_{eo}(\boldsymbol{t} \cdot \nabla \phi)$, $\boldsymbol{n} \cdot \boldsymbol{J}_i = 0$, $i = 1,...,N$, (5')

where t is the matrix containing vectors spanning the tangential plane of the solid surface. The boundary condition containing the electroosmotic mobility μ_{eo} is the von Smoluchowski equation.

Model equations were discretized on the rectangular (in 2D) or cubic (in 3D) grid and processed by the finite element method and resulted in the set of linear and non-linear equations. This set of equations was solved by the Newton method and the system

342 L. Seda and J. Kosek

of linear equations solved during each iteration was solved by the LU decomposition of the banded matrix in 2D or by the multigrid algorithm in 3D [7].

4. Electroosmotic flow in porous media with negligible Debye length

The distribution of the fluid velocity, pressure and electric potential in the spatially 2D porous structure with the assumption of the negligible thickness of the electric double layer was computed. The system was described by the set of equations (1'), (2') and (4) with boundary conditions (5') applied on the surface of the solid phase. Periodic boundary conditions were employed on the lower and upper boundary in Figure 2a. Boundary conditions on the left and right boundary are also considered to be periodic,

$$p_{\text{right}} - p_{\text{left}} = \Delta p$$
, $\phi_{\text{right}} - \phi_{\text{left}} = \Delta \phi$, $c_{i,\text{right}} - c_{i,\text{left}} = 0$, (7)

for i=1,...,N. The obtained solution is visualized on Figure 2 for a spatially 2D domain with a coarse discretization. In the finite element method bilinear base functions are used for state variables $\{p, \phi, c_i\}$, but biquadratic base functions are employed for v. Multigrid algorithm performs well in 3D and computations with reconstructed porous media larger than $100 \times 100 \times 100$ voxels are feasible on personal computers, cf. Figure 2b.

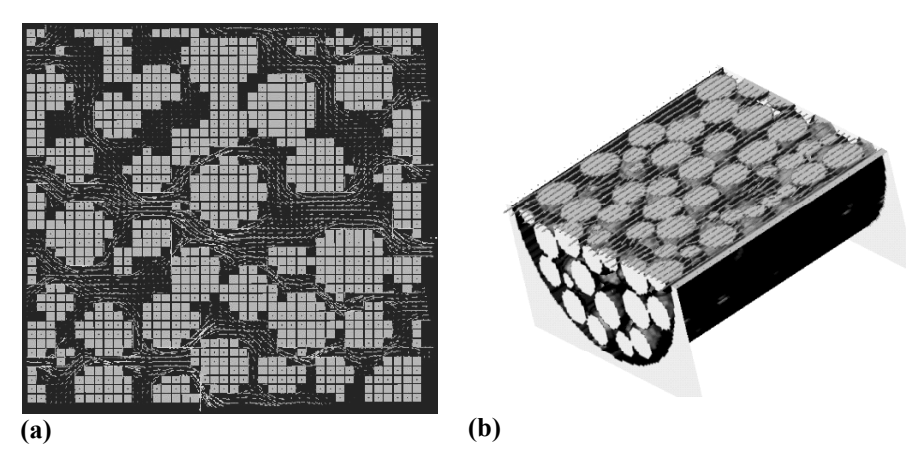


Figure 2. Electroosmotic flow in spatially 2D and 3D porous domains ($\Delta p = 0$, $\Delta \phi > 0$). Arrows represent the velocity distribution. (a) The size of the considered domain is $10 \times 10 \text{ }\mu\text{m}$.

5. Ionic permselectivity in a narrow capillary and in a porous medium

The concentration polarization can develop in the case of the Debye length comparable with the pore diameter. It is demonstrated in Figure 3 for the simple case of migration of ions through the spatially 2D microchannel with a nonuniform distribution of surface charge density σ ,

$$\sigma = \begin{cases} -5 \times 10^{-5} \text{ C/m}^2 & \text{for } x \in \langle 0.67, 1.33 \rangle \mu\text{m} \\ 0 \text{ C/m}^2 & \text{for } x \notin \langle 0.67, 1.33 \rangle \mu\text{m} \end{cases}$$

The intensity of the externally applied electric field is $E = |-\nabla \phi| = 150 \text{ kV/m}$. Concentration of the uni-univalent electrolyte on the left and on the right boundary is $c_{\text{left}} = c_{\text{right}} = 0.001 \text{ mol/m}^3$. The considered system is described by eqs (1)–(4) and applied boundary conditions are (5) and (6). Co-ions migrate from left to right due to

the externally applied potential difference, cf. Figure 3b. Because of the electric repulsion between the negatively charged ions and negatively charged walls of the channel the co-ions with concentration c_- accumulate at x < 0.67 µm in front of the charged part. The concentration of counter-ions c_+ increases in the middle part of the capillary due to the attractive interaction with the wall, cf. Figure 3a. The ratio of molar fluxes (selectivity) of counter-ions to co-ions is $J_+/J_-=1.69$.

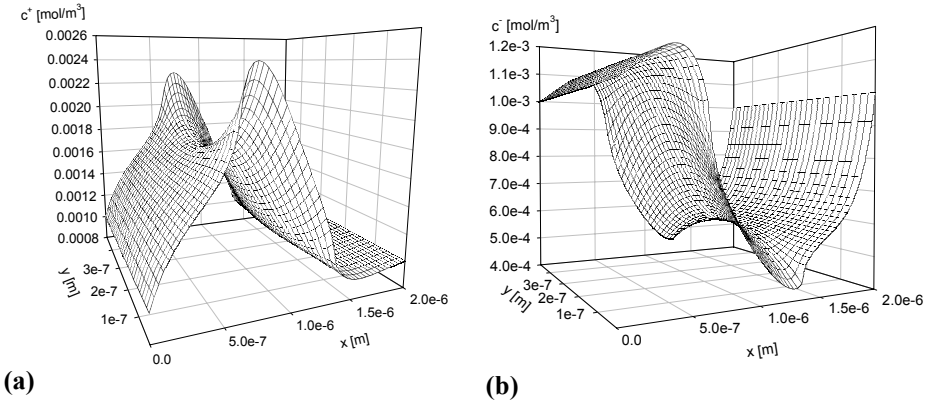
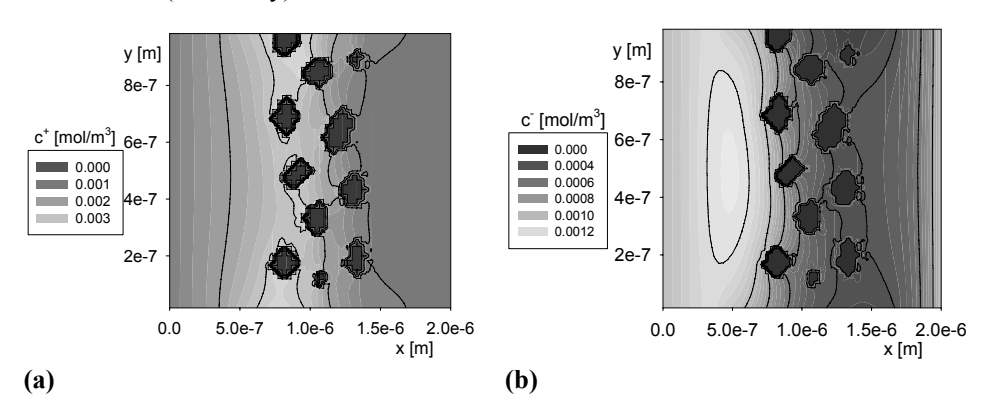


Figure 3. Distribution of ionic concentration in the spatially 2D microchannel: a) counter-ions c_+ ; b) co-ions c_- .

The concentration distribution in the narrow micro-channel containing charged particles with the surface charge density $\sigma = -2 \times 10^{-5}$ C/m² subjected to the externally applied electric field E = 150 kV/m is displayed in Figure 4. The surface charge distribution on the walls of the micro-channel is

$$\sigma = \begin{cases} -2 \times 10^{-5} \, \text{C/m}^2 & \text{for } x \in \left\langle 0.47, 1.67 \right\rangle \mu\text{m} \\ 0 \, \text{C/m}^2 & \text{for } x \notin \left\langle 0.47, 1.67 \right\rangle \mu\text{m} \end{cases}$$

The concentration of the uni-univalent electrolyte on the left and on the right boundary is $c_{\text{left}} = c_{\text{right}} = 0.001 \text{ mol/m}^3$. Negatively charged co-ions migrate from the left to the right part of the micro-channel. The middle part of the micro-channel containing charged particles is depleted of co-ions and enriched by counter-ions because of electrostatic interactions with charged surfaces. The concentration polarization develops due to the accumulation of negatively charged co-ions at $x < 0.47 \,\mu\text{m}$. The ratio of molar fluxes (selectivity) of counter-ions to co-ions is $J_+/J_- = 2.47$.



344 L. Seda and J. Kosek

Figure 4. Distribution of ionic concentration in the spatially 2D microchannel filled with charged particles: a) counter-ions c₊; b) co-ions c₋.

6. Conclusions

The principal parameters of the porous media (e.g., membranes) that affect their performance in electric field driven applications are: (i) spatially 3D structure of the porous media, (ii) type and distribution of fixed charged groups in the porous structure, and (iii) type and concentration of the electrolyte. The fixed charge groups in the membrane cause the excess of counter-ions and the exclusion of co-ions in the pores. However, the absolute concentration of the fixed charge itself is not relevant for the permselectivity of the membrane. Most current modeling studies describe the transport processes in porous media represented either as simplified geometrical structures (e.g., cylindrical capillaries), or as effective-scale (i.e., space-averaged) pseudo-homogeneous media. We have developed the software allowing to predict the transport and separation properties of porous medium (e.g., perfusion flow and ionic permselectivity) from its micro-structure in applications involving electrodialysis, capillary electrochromatography and nanofiltration [8–11].

Porous materials in electric field applications are either polymeric, anorganic or mixed polymeric/anorganic in their chemical nature. These materials very often exhibit a broad pore size distribution and contain pores in the range of 1 nm to 100 μ m. Multiscale modeling of electric field driven processes in porous media with a broad pore size distribution is the next objective of our work. Another objective of our ongoing work is the automatic refinement of the computational grid required to solve problems with the Debye length significantly smaller than the average pore size but still large enough to prevent the use of the von Smoluchowski boundary condition.

Acknowledgments. The support from the Czech Grant Agency (project 104/03/H141) and from the Ministry of Education (MSM 6046137306) is acknowledged.

References

- 1. Mario, S., Coelho, D., Bekri, S., Adler, P.M.: J-Col. Int. Sci. 223, 296-304-(2000).
- 2. Grimes, B.A., Mayers, J.J., Liapis, A.I.: *J. Chrom. A* **890**, 61-72 (2000).
- 3. Vallano, P.T., Remcho, V.T.: Anal. Chem. 72, 4255-4265 (2000).
- 4. Adler P.M.: Porous Media: Geometry and transports. Butterworth-Heinemann, Boston (2001).
- 5. Kosek J., Stepanek F., Marek M.: Modeling of transport and transformation processes in porous and multiphase bodies, in Advances in Chemical Engineering, Vol. 30 "Multiscale Analysis", edited by Marin G.B., Elsevier (2005).
- 6. Torquato S.: Random Heterogeneous Materials: Microstructure and Macroscopic properties. Sprinder/Verlag, New York (2002).
- 7. Holst M., Saied F.: J. Comput. Chem. 14, 105-113 (1993).
- 8. Delgado, Á.V.: Interfacial electrokinetics and electrophoresis. Marcel Dekker (2002).
- 9. Dongquing Li: Electrokinetics in Microfluidics. Elsevier Academic Press (2004).
- 10. Paces M., Kosek J., Marek M., Tallarek U., Seidel-Morgenstern A.: Electrophoresis 24, 380-389 (2003).
- 11. Paces M., Kosek J., Kubicek M., Marek M.: Modeling of the perfusion flow in capillary electrochromatography, submitted (2005).